FINITE ELEMENT ANALYSIS OF MODE-I STEADY CRACK GROWTH IN PLANE STRESS

Luo Xuefu (罗学富)
Tsinghua University, China
Zhang Xiaoti (张晓堤)
Institute of Mechanics, Academia Sinica, China
Hwang Kehchih (黄克智)
Tsinghua University, China

INTRODUCTION

Up to now the near-tip fields for elastic-plastic crack growth have been studied relatively fully for mode-III problems and for elastic-perfectly plastic material. For this material Slepyan[1], Gao[2] and Rice et al.[3] have obtained the near tip fields for the mode-I steady crack growth in plane strain. For power hardening material, the near-tip asymptotic steady state solution has been obtained by Gao, Zhang and Hwang[4,5] for mode-III and by Gao and Hwang[6] for mode-I in plane strain (with $\nu=\frac{1}{2}$). But no solution is obtained for mode-I in plane stress in case of power hardening or nonhardening materials.

In a finite element analysis for mode-III and mode-I steady crack growth in plane strain, Dean and Hutchinson[7] adopted a mesh moving with the crack-tip. Here based upon the J_2-flow theory, the method is adapted to the analysis of mode-I problem in plane stress under small scale yielding.

FINITE ELEMENT ANALYSIS

All quantities are nodimensionalized and denoted by a bar "-". The nondimensional coordinates, displacements, stresses and strains are

$$\bar{x} = x/(K/\sigma_0)^2 \quad \bar{y} = y/(K/\sigma_0)^2 \quad \bar{r} = r/(K/\sigma_0)^2$$
$$\bar{u} = u/(K^2/G\sigma_0) \quad \bar{v} = v/(K^2/G\sigma_0)$$
$$\bar{\sigma}_x = \sigma_x/\sigma_0 \quad \bar{\sigma}_y = \sigma_y/\sigma_0 \quad \bar{\tau}_{xy} = \tau_{xy}/\sigma_0 \tag{1}$$
$$\bar{\varepsilon}_x = G\varepsilon_x/\sigma_0 \quad \bar{\varepsilon}_y = G\varepsilon_y/\sigma_0 \quad \bar{\gamma}_{xy} = G\gamma_{xy}/\sigma_0$$

respectively, where k — stress intensity factor, σ_0— yield stress and G — shear modulus.

The material hardening is characterized by

$$\bar{\sigma}_e^{1/N} = \bar{\sigma}_e = 3\bar{\varepsilon}_e^p \tag{2}$$

where $\bar{\sigma}_e$ — the equivalent stress, $\bar{\varepsilon}_e^p = \int d\bar{\varepsilon}_e^p$— the equivalent plastic strain, and N — the hardening exponent.

The variational equation of static equilibrium is

$$\int\{\bar{\sigma}\}^T\delta\{\bar{\varepsilon}\}d\bar{A}=\int\{\bar{f}\}^T\delta\{\bar{u}\}d\bar{s} \tag{3}$$

in which $\{\bar{f}\}$ denotes the surface load. Using Hooke's law

$$\{\bar{\sigma}\} =[\bar{D}^e](\{\bar{\varepsilon}\} - \{\bar{\varepsilon}^p\}) \tag{4}$$

and after finite element discretization, we obtain the nodal equation of equilibrium

$$[\bar{K}^e]\{\bar{U}\} = \{\bar{F}\} + \{\bar{F}^p\} \tag{5}$$

where $[\bar{K}^e]$ — the matrix of structure's elastic rigidity, $\{\bar{U}\}$ — the vector of nodal displacements, $\{\bar{F}\}$ — the nodal surface load, and $\{\bar{F}^p\}$ — the equivalent plastic nodal load. Eq. (5) has to be solved by iteration, since $\{\bar{F}^p\}$ depends on plastic strain $\{\bar{\varepsilon}^p\}$, which is unknown prior to solution.

The finite element mesh is shown schematically in Fig. 1, in which each of quadrilateral contains two contant strain triangular elements. The middle point of common side of two neighboring triangles is called the "optimal stress point". The stresses at a "optimal stress point" in plastic region are determined by integration along the negative $\bar{x}$-direction over

the history described by all of the "optimal stress points" at the same height $\bar{y}$ and to the right of the point considered.

The dimensions of the region for computation are taken as: $\bar{x}_D = 7.2$, $\bar{x}_A = -6.0$, $\bar{y}_B = 8.64$. The mesh consists of 4183 triangular elements, with 4374 degrees of freedom, The nondimensional size of the near-tip smallest element is 0.002, which for nonhardening case is 0.7% of the distance to the elastic-plastic boundary ahead of the crack on the $\bar{x}$-axis (i.e. size of plastic region in $\bar{x}$-direction). The region for computation is more than 25 times larger than the size of plastic region. Comparison of the results which are obtained for different varying sizes taken for the region, shows that our region is big enough so that the small scale yielding condition be approximately fulfilled.

The tractions on the boundaries AB, BC and CD are derived from the elastic singular K-field

$$\bar{\sigma}_{ij} = f_{ij}(\theta)/\sqrt{2\pi\bar{r}} \tag{6}$$

The incremental constitutive relations are

$$\{\Delta\bar{s}\} = 2([I] - \frac{3}{\bar{\zeta}+3}\{n\}\{n\}^T)\{\Delta\bar{e}\} \tag{7}$$

where $\{\Delta\bar{s}\}$ — the stress deviator increment, $[I]$ — 4×4 unit matrix, $\{\Delta\bar{e}\}$— strain deviator increment, $\{n\}$ — the unit vector normal to the yield surface in stress-space, and $\bar{\zeta} = \Delta\bar{\sigma}_e / \Delta\bar{\varepsilon}_e^p$ — slope of the hardening curve, for nonhardening material $\bar{\zeta} = 0$. $\{\Delta\bar{s}\}$ and $\{\Delta\bar{e}\}$ are

$$\begin{aligned}\{\Delta\bar{s}\}^T &= \{\Delta\bar{\sigma}_x-\Delta\bar{\sigma}_m,\ \Delta\bar{\sigma}_y-\Delta\bar{\sigma}_m,\ -\Delta\bar{\sigma}_m,\ \sqrt{2}\bar{\tau}_{xy}\}\\ \{\Delta\bar{e}\}^T &= \{\Delta\bar{\varepsilon}_x-\Delta\bar{\varepsilon}_m,\ \Delta\bar{\varepsilon}_y-\Delta\bar{\varepsilon}_m,\ \Delta\bar{\varepsilon}_z-\Delta\bar{\varepsilon}_m,\ \bar{\gamma}_{xy}/\sqrt{2}\}\end{aligned} \tag{8}$$

respectively, here $\Delta\bar{\sigma}_m$ and $\Delta\bar{\varepsilon}_m$ denote the mean stress increment and the mean strain increment, respectively.

The final state of each increment step is required to fall exactly on the material hardening curve. Following Rice and Tracey[8], this requirement is satisfied for nonhardening material by taking

$$\{n\} = \frac{\{\bar{s}_1\}+\{\Delta\bar{e}\}}{|\{\bar{s}_1\}+\{\Delta\bar{e}\}|} \tag{9}$$

where $\{s_1\}$ is the stress deviator of the initial state of the increment step considered. For hardening material, this requirement, i.e.,

$$(\bar{\sigma}_e+\Delta\bar{\sigma}_e)^{1/N} - (\bar{\sigma}_e+\Delta\bar{\sigma}_e) = 3(\bar{\varepsilon}_e^p+\Delta\bar{\varepsilon}_e^p) \tag{10}$$

can be satisfied by taking $\{n\}$ the same as (9), and $\bar{\zeta}$ to be

$$\bar{\zeta} = \frac{3\Delta\bar{\sigma}_e}{\sqrt{6}\{n\}^T\{\Delta\bar{e}\}-\Delta\bar{\sigma}_e} \tag{11}$$

where the equivalent stress increment

$$\Delta\bar{\sigma}_e = (\bar{\sigma}_e^{1/N} + \sqrt{6}\{n\}^T\{\Delta\bar{e}\})^N - \bar{\sigma}_e \tag{12}$$

For plane stress, only $\bar{\varepsilon}_x$, $\bar{\varepsilon}_y$ and $\bar{\gamma}_{xy}$ can be determined from inplane displacements $\bar{u}$ and $\bar{v}$, with $\bar{\varepsilon}_z$, and hence $\{\Delta\bar{e}\}$ in (8) undetermined. In view of this difficulty, which does not exist for plane strain, we iterate the mean strain $\bar{\varepsilon}_m$ together with displacements $\{\bar{U}\}$, with $\bar{\varepsilon}_m$ determined in each increment step by the relation of volumetric deformation

$$\bar{\varepsilon}_m = -\frac{1-2\nu}{2(1+\nu)}\bar{s}_z \tag{13}$$

Computation is made for materials with ten values of N, namely, N=0.9, 0.8,..., 0.1, 0. Beginning from the elastic material (n=1), the solution of higher hardening case is successively used to start the iteration for next lower hardening case.

The error of two consecutive (i-1)-th and i-th iterations is estimated by

$$\varepsilon^{(i)} = \max_{1\le j\le n}\left(\frac{\left|U_j^{(i)}-U_j^{(i-1)}\right|}{\left|U_j^{(i)}\right|+1}\right) \tag{14}$$

here n is the number of degrees of freedom. The convergence is considered satisfactory when $\varepsilon^{(i)} \le 0.0004$. The number of iterations required is about 10 for materials with large N, and about 30 for elastic-perfectly plastic material.

RESULTS AND DISCUSSION

(1) The variation of the geometry of the active plastic zone with hardening exponent N is shown in Fig. 2. In contrast to mode I in plane strain[7], in the case of plane stress, the geometry depends upon N significantly. The less hardening the material is, the smaller the dimension of active plastic zone in $\bar{y}$-direction and the bigger in $\bar{x}$-direction will be. No secondary plastic zone is found.

(2) The angular distribution of near-tip stresses for elastic-perfectly plastic materials is shown in Fig. 3. The distribution of σ_y and τ_{xy} is somewhat similar to that for plane strain[7], but σ_x changes sign at θ near 160°.

(3) For elastic-perfectly plastic material, the distributions of near-tip strain $\bar{\varepsilon}_y$ along the lines of $\theta = 0$ and $\theta = \frac{\pi}{2}$ are shown in Fig. 4. They are nearly straight lines in semi-logarithmic plot. This seems to hint, in contrast to the modified Prandtl field for plane strain crack growth, directly ahead of the crack is a sector-zone with strain singularity, rather than a uniform stress region.

(4) By curve fitting based upon displacements obtained for 19 nodes on the crack flanks, the 45° COD values defined by Rice (see Tracey[9]) are determined. The results are shown in Fig. 5. The corresponding 45° COD values have been obtained by Shih[10] for stationary cracks with HRR singularity. A COD-based fracture criterion is used, and the ratios of stress intensity factor K_{ss} needed to drive the crack in steady state to K_c at initiation are determined. As shown in Fig. 6, the ratios K_{ss}/K_c vary strongly with the material constant σ_0/G and the hardening exponent N, especially at the neighborhood of N = 0.

CONCLUSION

(1) For mode-I crack growth in plane stress, the geometry of the active plastic zone depends upon the hardening exponent N significantly.

(2) The near-tip fields for mode-I crack growth in plane stress seem to be quite different from the modified Prandtl fields for plane strain.

(3) The lower the exponent N, or the smaller the yielding strain σ_0/G is, the higher will be the ratio K_{ss}/K_c, hence the larger will be the resistance to crack growth and the longer the stable crack growth will last.

REFERENCES

[1] Slepyan, L.I., Izv. Akad. Nauk SSSP, MTT, 11 (1976), 144.

[2] Gao Yuchen, Acta Mecanica Sinica, 1 (1980), 48 (in Chinese with English abstract).

[3] Rice, J.R., Drugan, W.J. and Sham, T.L., ASTM STP 700.

[4] Gao Yuchen, Zhang Xiaoti and Hwang Kehchih, to appear in the "International Journal of Fracture".

[5] Gao Yuchen, Zhang Xiaoti and Hwang Kehchih, Acta Mechanica Sinica, 5 (1981), 452 (in Chinese with English abstract).

[6] Gao Yuchen and Hwang Kehchih, ICF5, Cannes, France (1981).

[7] Dean, R.H. and Hutchinson, J.W., ASTM STP 700.

[8] Rice, J.R. and Tracey, D.M., Computational Fracture Mechanics, in Numerical and Computer Methods in structural Mechanics (1973), 585.

[9] Tracey, D.M., Trans. ASME, J. Engng. Materials and Technol., 98 (1976), 146.

[10] Shih, C.F., J. Mech. Phys. Solids, Vol. 29, No. 4 (1981), 305.

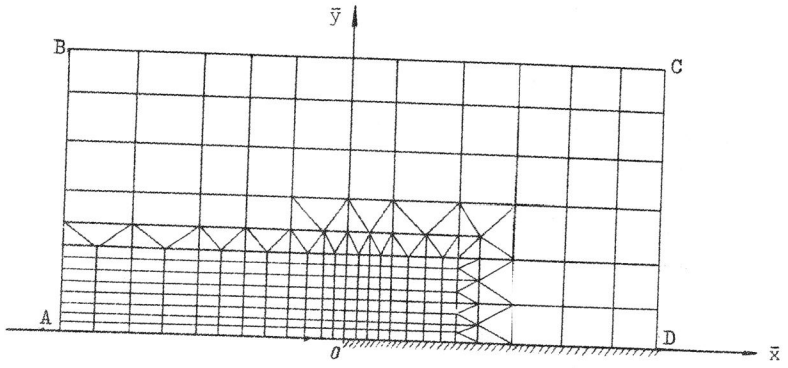

Fig. 1 Coarse representation of finite element grid

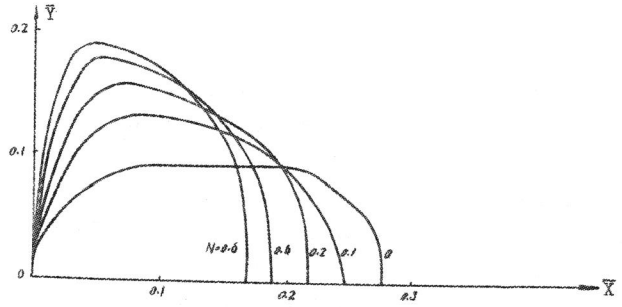

Fig. 2 Variation of the plastic zone with exponent N

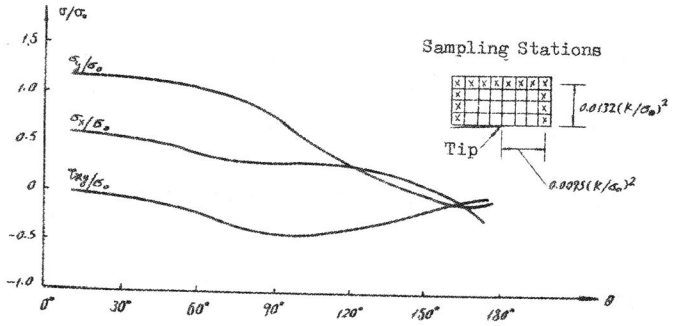

Fig. 3 Angular distribution of near-tip stresses for elastic-perfectly plastic material

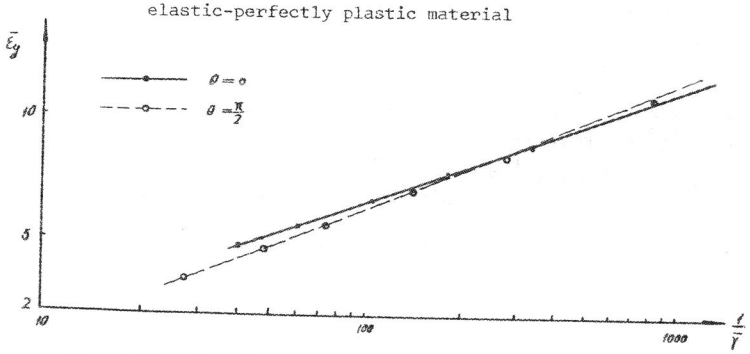

Fig. 4 The distribution of near-tip strain $\bar{\varepsilon}_y$ for elastic-perfectly plastic material

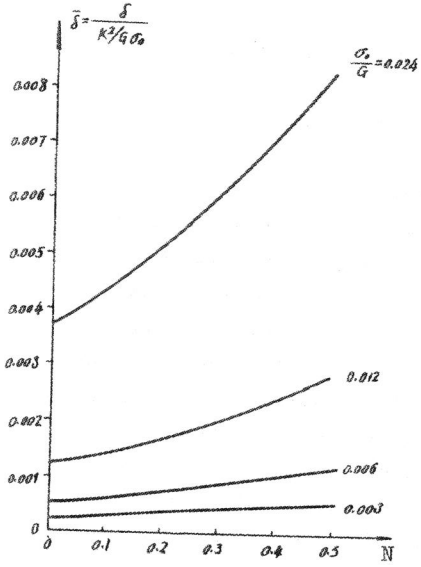

Fig. 5 Variation of COD with σ_0/G and N

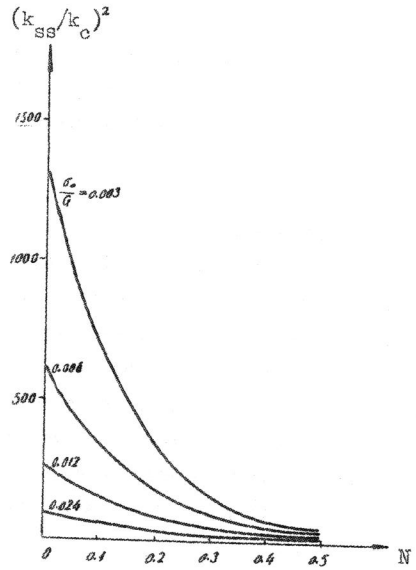

Fig. 6 Variation of K_{ss}/K_c with σ_0/G and N